Hindawi Publishing Corporation
Journal of Nanomaterials
Volume 2015, Article ID 579349, 6 pages
http://dx.doi.org/10.1155/2015/579349

Research Article

Noninvasive 3D Structural Analysis of Arthropod by Synchrotron X-Ray Phase Contrast Tomography

Shengkun Yao, Yunbing Zong, Jiadong Fan, Zhibin Sun, and Huaidong Jiang

State Key Laboratory of Crystal Materials, Shandong University, Jinan 250100, China

Correspondence should be addressed to Huaidong Jiang; hdjiang@sdu.edu.cn

Received 16 October 2015; Accepted 17 December 2015

Academic Editor: Jim Low

X-ray imaging techniques significantly advanced our understanding of materials and biology, among which phase contrast X-ray microscopy has obvious advantages in imaging biological specimens which have low contrast by conventional absorption contrast microscopy. In this paper, three-dimensional microstructure of arthropod with high contrast has been demonstrated by synchrotron X-ray in-line phase contrast tomography. The external morphology and internal structures of an earthworm were analyzed based upon tomographic reconstructions with and without phase retrieval. We also identified and characterized various fine structural details such as the musculature system, the digestive system, the nervous system, and the circulatory system. This work exhibited the high efficiency, high precision, and wide potential applications of synchrotron X-ray phase contrast tomography in nondestructive investigation of low-density materials and biology.

1. Introduction

X-ray imaging techniques exhibit noticeable advantages in the study of morphology and internal microstructures in biology, owing to the high penetrating power and short wavelength of X-rays [1–3]. Among the various X-ray imaging techniques, phase contrast X-ray microscopy suit the imaging of biological specimens which show low contrast by conventional absorption contrast microscopy [4, 5]. Phase contrast microscopy is based on the Fresnel diffraction theory, providing high contrast images by using the phase shift of the X-ray. Both the amplitude and the phase of X-ray are changed when X-rays pass through objects. This change can be characterized by the complex refractive index $n = 1 - \delta + i\beta$, where $\delta = r_e \rho_e \lambda^2 / 2\pi$ and $\beta = \mu\lambda/4\pi$. δ and β are correlated with the phase shift and the absorption properties, respectively [1]. For low-Z materials such as soft tissues imaged with high energy X-ray, phase variations can be two to three orders of magnitude larger than the absorption ones, and an increased image contrast can be achieved [6]. Therefore, phase contrast microscopy could significantly improve the image quality of biological sample in comparison to conventional absorption-based X-ray microscopy. So far, various X-ray phase contrast methods have been developed with the advancement of synchrotron radiation facility worldwide, including propagation-based or in-line imaging [7–9], X-ray interferometry [10], analyzer-based or diffraction-enhanced imaging [11], and grating-based imaging and grating noninterferometric methods [12]. A large number of X-ray phase contrast imaging results have been reported on both technical developments and biomedical applications [2, 3, 9–11, 13–15]. Three-dimensional imaging can be realized by the combination with computed tomography.

In this paper, we demonstrated the ability of 3D image analysis to identify fine structural details of an earthworm by synchrotron X-ray in-line phase contrast tomography. Earthworms, tube-shaped and segmented, refer to a specific group of invertebrates within the phylum Annelida [16, 17]. They are commonly found living in soil, feeding on live and dead organic matter, and contributing to enriching and improving soil for plants and animals [18]. Traditionally, the microstructures can be achieved by histological section, in which serial sections are stained and observed by light microscopy or scanning and transmission electron microscopy. However, the anatomical approaches are

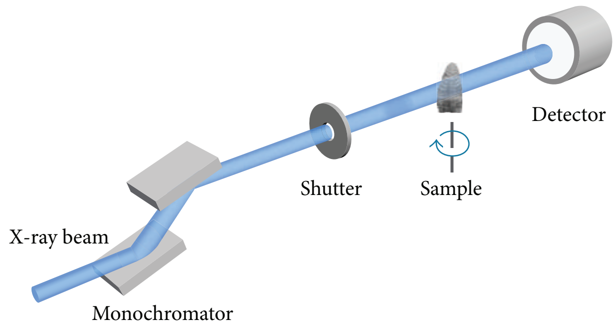

Figure 1: Schematic diagram of the synchrotron X-ray in-line phase contrast imaging setup. A monochromatic X-ray with specific energy is selected by a monochromator from the synchrotron radiation X-ray beam. Fresnel diffraction occurs on the interfaces of different tissues when the beam passes through the sample. The phase contrast image is recorded by a detector when the detector and the sample are at an appropriate distance. During the tomographic scan, the specimen is rotated around the vertical axis at 180 degrees. In this experiment a mechanical shutter is used to avoid radiation damage of biological sample in the absence of image capture.

destructive and time consuming, making measurements of large numbers of samples impractical. Here, we used in-line phase contrast X-ray tomography, the simplest and the most straightforward among all types of the phase contrast microscopy, to noninvasively investigate the external morphology and internal microstructures, by which we hope to significantly advance the understanding of the species and the evolution.

2. Materials and Methods

The experiment was performed on X-ray imaging and biomedical application beamline (BL13W1) at Shanghai Synchrotron Radiation Facility (SSRF) [19, 20]. The schematic diagram of the in-line phase contrast microscopy system is shown in Figure 1. During the experiment, a collimated X-ray beam with energy of 12 keV was optimized, by which an improved image contrast enhancement was achieved benefiting from the phase shift of X-rays. The sample used for the experiment is a dehydrated earthworm, which was dried with critical point drier to maintain the microstructure unchanged. The earthworm was mounted on a rotation stage and placed in the X-ray beam path. When X-ray beams traveled through the sample, the downstream beams carried the absorption and phase shift information. After propagating a distance of 8.5 cm, the phase shifts in the downstream beams are transformed into measurable intensity variations by Fresnel diffraction. An X-ray-sensitive CCD camera with maximum of 2048×2048 pixels was used to transform the beams to images with effective $3.7 \times 3.7\,\mu$m pixel resolution. All 2D projections measured from the samples were saved as TIFF format images. The specimen was rotated around its cylinder axis for 180° during the data acquisition. The number of projections (N) is determined by $N \sim \pi D/(2P)$, where D is the thickness of the sample and P is the detector pixel size, to achieve an acceptable spatial resolution [11]. The projections were acquired at a single distance. The number of projections is 450, and the exposure time is 6 s for each projection. Before the image acquisition, a calibration process was strictly performed to make the sample rotating platform axis parallel to the CCD camera. During the image acquisition, white field images were measured at ninety tomographic image intervals with the X-rays on but without the samples in the beam. Five dark field images, without the X-rays in the beam, were also acquired at the end of the data acquisition. The phase retrieval of 2D images and the tomographic reconstruction including background correction, rotating axis position correction, and filtered back projection reconstruction were carried out by a CT reconfigurable software compiled by the BL13W1 experimental station [21–23]. Subsequently, the three-dimensional images of the sample were visualized with Amira software.

3. Results and Discussion

We demonstrated in-line phase contrast tomography of an earthworm. Figure 2 shows a representative projection, in which only the region of interest is imaged. The intensity of the measured projection in Figure 2(a) corresponds to the second derivative of the refractive index [2]. In this case, the interfaces of different organs are enhanced, and qualitative details such as overall size of different structures can be observed. In order to perform quantitative analysis of different organs by mass density, phase retrieval of the measured projections was carried out with a single sample-to-detector distance [23]. As shown in Figure 2(b), the intensity of retrieved projection corresponds to the index of refraction. Subsequently, the two sets of projections before and after phase retrieval were reconstructed separately by using the filtered back projection algorithm. The intensity of the direct reconstructed tomogram without phase retrieval is the mixture of three parts, including the 3D map of the second derivative of the refractive indices, the 3D map of linear attenuation coefficients, and the artifacts related to the global distribution of the attenuation coefficients and refractive indices [24, 25]. Figure 3(a) shows one representative direct reconstructed slice, in which the interfaces of different tissues are enhanced and distinguishable. However, it is difficult to accurately determine different organs with the distribution of the density, and the slice is also corrupted by noises as shown in Figure 3(c) (rectangular region in Figure 3(a)). While the intensity of the tomogram reconstructed from projections with phase retrieval represents the 3D distribution of the refractive index, by which the precise interior structures of earthworm can be easily identified (Figure 3(b)), the zoomed-in region (Figure 3(d)) shows a much higher signal to noise ratio. In consideration of the features of the tomograms before and after phase retrieval, we performed the further structural analysis with the tomograms after phase retrieval.

Synchrotron X-ray phase contrast tomography provides an ideal image technique for visualizing internal microstructures with different mass densities. Here it also shows high efficiency in the investigation of the earthworm, by which not only the external morphology but also the internal

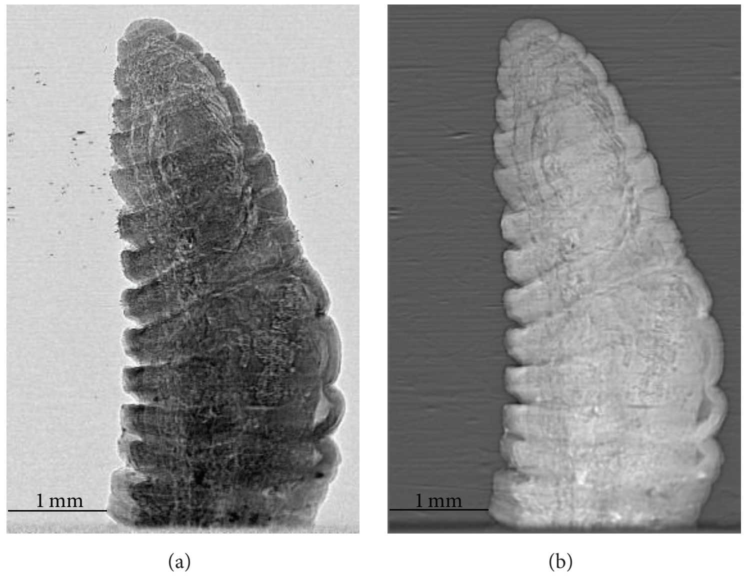

Figure 2: A representative projection before (a) and after (b) phase retrieval. The measured intensity in (a) corresponds to the second derivative of the refractive index. The qualitative details such as overall size of different structures can be observed due to enhancement of the interfaces between different organs. The intensity in (b) corresponds to the index of refraction, by which quantitative analysis such as identification of different organs by mass density can be carried out after tomographic reconstruction (scale bars, 1 mm).

microstructures were nondestructively achieved with sufficient spatial resolution. Figure 4 shows the head part of the earthworm, which indicates the 3D morphology in ventral, lateral, and dorsal views. The earthworm shows a streamlined and tube-shaped body and is divided into segments. The furrows on the surface of the body can be observed clearly. Synchrotron X-ray phase contrast tomography allows sectioning virtually in any directions in the native state (Figure 5). The transverse cross sections (Figure 5(i, ii, iii, and iv)) show complex internal structures of the earthworm with high contrast. The earthworm is covered by thin cuticles (labeled in Figure 5(ii)). Then two layers of muscles are under the epidermis, a thin outer layer of circular muscle and a much thicker inner layer of longitudinal muscle, enabling the worm to move forward. What is more, the setae, which help anchor and control the worm when moving through soil, are observed in the body (Figure 5(iii)). The region interior to the muscle layer is the coelom which is the fluid-filled chamber to maintain the body structure. The digestive system, which runs straight through the body without coiling, is at the center of the coelom. And it is surrounded above and below by the dorsal blood vessel and the ventral blood vessel. The ventral nerve cords, surrounded in each segment by a pair of blood vessels, are also observed at different slices (Figure 5(iii)).

Earthworms play a critical role in our planet's ecosystem by decomposing organic material into nutrient-rich soil. Since earthworms digest organic matter in the soil, worm castings provide a perfect mix of nutrients that are available to the plants. Besides, the special body structure makes earthworms tunnel through the soil, which increases soil porosity. These characteristic biological functions of earthworms are closely correlated with their microstructures. The characteristic external morphology (streamlined and segmented body) and internal structures make an adaptation to living in narrow burrows underground. The structural details of the earthworm are in excellent agreement with that achieved by histological sections [16, 17]. In comparison with the histological methods that are often technically difficult and labor intensive, synchrotron X-ray phase contrast tomography shows high efficiency and high precision in the noninvasive structural analysis of the earthworm. The structural integrity is crucial to investigate the relationship of structures and functions in biology. Three-dimensional image techniques taking advantage of the high penetration of X-rays provide nondestructive methods in comparison to the conventional histological method in which sectioning is essential. Even though some other techniques, such as MRI, confocal microscopy, and ultrasound imaging, could provide noninvasive methods, these tools are often limited by sample size or spatial resolution [26–28]. While the spatial resolution in phase contrast X-ray imaging is mainly limited by detectors, images of thick samples can be achieved. Thus, much finer microstructures of the earthworms can be observed with higher-resolution detectors. Moreover, the efficiency is significantly improved in comparison with histological methods. The overall time in our study including experiment, tomographic reconstruction, and postdata analysis is limited to 1~2 hours. The improved efficiency makes quick analysis of large numbers of samples possible. Besides, without staining, different tissues of the sample can be distinguished by characteristic refractive indexes in phase contrast X-ray tomography, which contributes to obtaining a better understanding of the microstructures of earthworm. In addition, due to the high intensity of X-ray source, synchrotron X-ray in-line phase contrast imaging makes dynamic studies possible. Phase contrast X-ray tomography

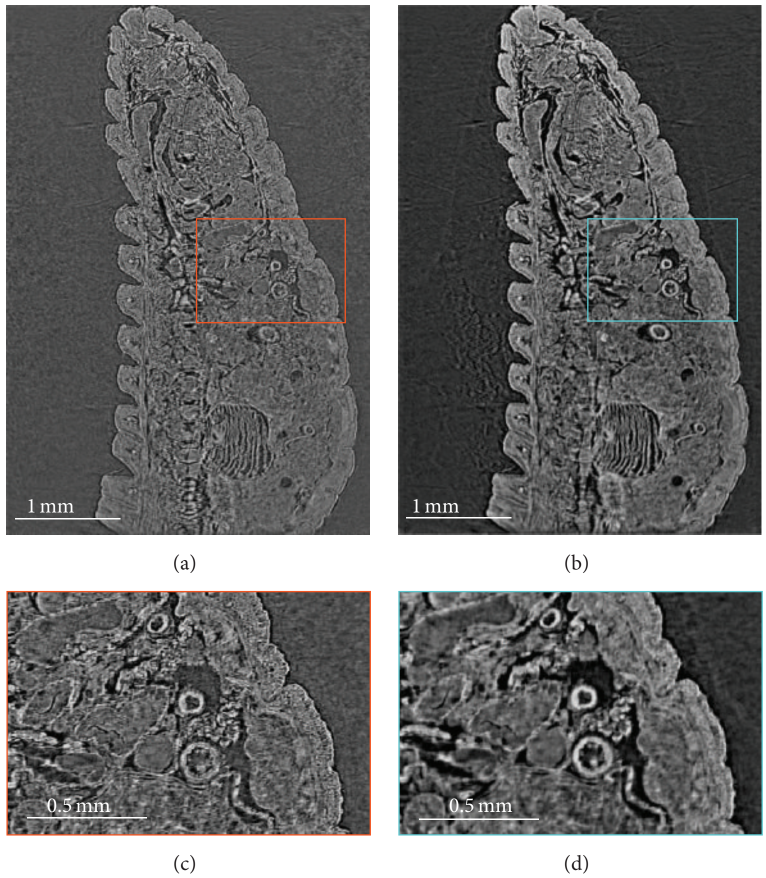

Figure 3: Representative tomographic slices reconstructed from projections with and without phase retrieval. In the directly reconstructed tomographic slice (a), the interfaces of different tissues are distinguishable. However, accurate determination of different organs with the distribution of density is difficult. In the slice reconstructed with projections after phase retrieval (b), the precise interior structures of earthworm with characteristic mass density can be easily identified. The zoomed-in region (d) shows less noise and better image quality than (c) (scale bars in (a) and (b), 1 mm; in (c) and (d), 0.5 mm).

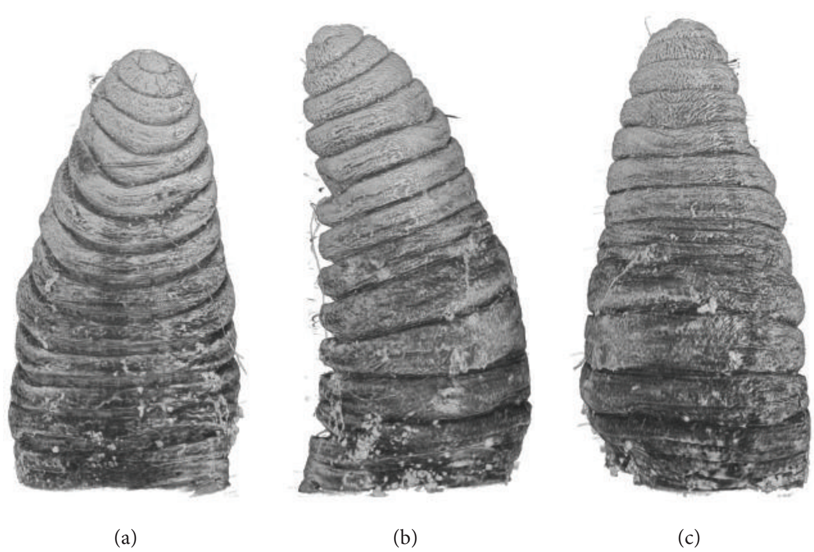

Figure 4: Volume rendering of the earthworm in ventral (a), lateral (b), and dorsal (c) views reconstructed with projections after phase retrieval. The earthworm with a streamlined and tube-shaped body is divided into segments, and the furrows can be observed clearly. The characteristic external morphology will be adapted to the living environment.

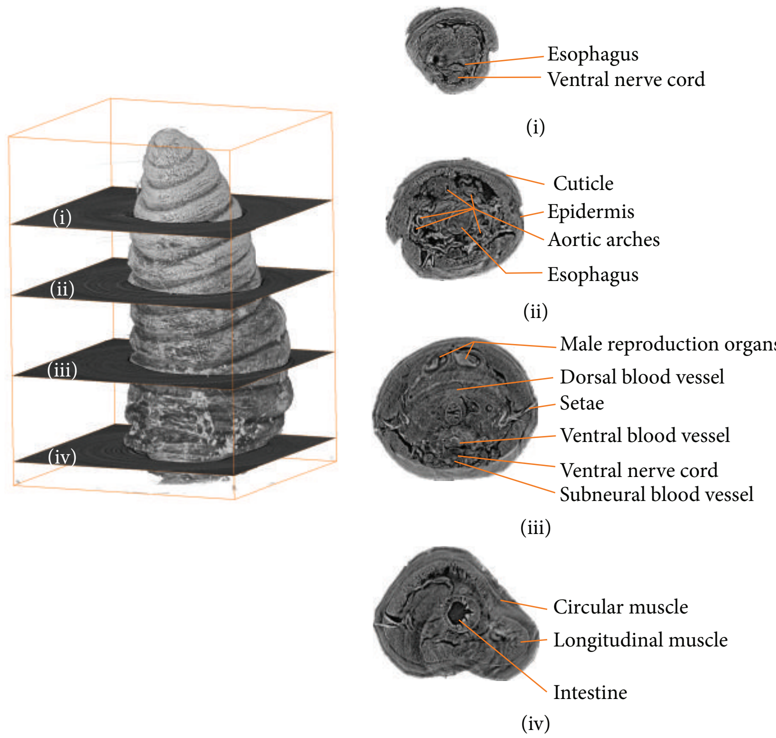

Figure 5: Identification of various interior organs by virtual sections. The musculature system, the circulatory system, nervous system, and the digestive system are observed, including longitudinal and circular muscles under the epidermis, setae under the cuticles, the dorsal and ventral blood vessels, the ventral nerve cords surrounded by blood vessels, and the intestine at the center of the coelom.

provides a useful supplementary analytical technique for conventional histological methods, which will have wider applications in biology.

4. Conclusion

In conclusion, we presented quantitative nondestructive 3D structural analysis of millimeter-sized arthropod with synchrotron X-ray phase contrast tomography. By comparison of tomographic reconstructions with and without phase retrieval, the external morphology and internal fine microstructures of the earthworm were quantitatively analyzed and discussed. We identified various structural details such as the musculature system, the circulatory system, nervous system, and the digest system. The physiological aspects contribute to the understanding of the morphological adaptation and the evolution. Our investigation demonstrated that phase contrast tomography has the potential advantages of reducing radiation dose and increasing accuracy over conventional X-ray imaging. Because overdose could lead to the radiation damage such as the change of biological microstructures, radiation dose is a primary consideration in the nondestructive 3D X-ray imaging of biological samples. In our experiment of phase contrast imaging based on the phase shift of high energy and high flux synchrotron X-rays, the radiation dose is relatively low in comparison to the conventional X-ray imaging. Furthermore, the radiation dose was decreased for in-line phase contrast imaging which can perform phase retrieval from images at a single sample-to-detector distance for biological samples. With the development of X-ray sources and use of high-resolution detectors, in-line phase contrast imaging technique has a wide range of potential applications, such as environment-dependent higher-resolution imaging and high-speed in situ tomography.

Conflict of Interests

The authors declare that there is no conflict of interests regarding the publication of this paper.

Acknowledgments

The authors thank the staff at Shanghai Synchrotron Radiation Facility for assistance with data acquisition. This work was supported by the Major State Basic Research Development Program of China (no. 2014CB910401) and the National Natural Science Foundation of China (31430031, 21390414, and U1332118).

References

[1] J. Als-Nielsen and D. McMorrow, *Elements of Modern X-Ray Physics*, John Wiley & Sons, 2011.

[2] Y. Liu, J. Nelson, C. Holzner, J. C. Andrews, and P. Pianetta, "Recent advances in synchrotron-based hard x-ray phase contrast imaging," *Journal of Physics D*, vol. 46, no. 49, Article ID 494001, 2013.

[3] M. W. Westneat, J. J. Socha, and W.-K. Lee, "Advances in biological structure, function, and physiology using synchrotron X-ray imaging," *Annual Review of Physiology*, vol. 70, pp. 119–142, 2008.

[4] T. J. Davis, D. Gao, T. E. Gureyev, A. W. Stevenson, and S. W. Wilkins, "Phase-contrast imaging of weakly absorbing materials using hard X-rays," *Nature*, vol. 373, no. 6515, pp. 595–598, 1995.

[5] S. W. Wilkins, T. E. Gureyev, D. Gao, A. Pogany, and A. W. Stevenson, "Phase-contrast imaging using polychromatic hard X-rays," *Nature*, vol. 384, no. 6607, pp. 335–338, 1996.

[6] A. Momose, T. Takeda, Y. Itai, and K. Hirako, "Phase-contrast X-ray computed tomography for observing biological soft tissues," *Nature Medicine*, vol. 2, no. 4, pp. 473–475, 1996.

[7] J. Zhang, D. Tian, R. Lin, G. Zhou, G. Peng, and M. Su, "Phase-contrast X-ray CT imaging of esophagus and esophageal carcinoma," *Scientific Reports*, vol. 4, article 5332, 2014.

[8] R. Tang, W.-X. Li, W. Huang et al., "CO_2-based in-line phase contrast imaging of small intestine in mice," *Scientific Reports*, vol. 3, article 2313, 2013.

[9] P. Cloetens, R. Mache, M. Schlenker, and S. Lerbs-Mache, "Quantitative phase tomography of Arabidopsis seeds reveals intercellular void network," *Proceedings of the National Academy of Sciences of the United States of America*, vol. 103, no. 39, pp. 14626–14630, 2006.

[10] I. Zanette, M. Bech, A. Rack et al., "Trimodal low-dose X-ray tomography," *Proceedings of the National Academy of Sciences of the United States of America*, vol. 109, no. 26, pp. 10199–10204, 2012.

[11] Y. Zhao, E. Brun, P. Coan et al., "High-resolution, low-dose phase contrast X-ray tomography for 3D diagnosis of human breast cancers," *Proceedings of the National Academy of Sciences of the United States of America*, vol. 109, no. 45, pp. 18290–18294, 2012.

[12] P. Zhu, K. Zhang, Z. Wang et al., "Low-dose, simple, and fast grating-based X-ray phase-contrast imaging," *Proceedings of the National Academy of Sciences of the United States of America*, vol. 107, no. 31, pp. 13576–13581, 2010.

[13] M. W. Westneat, O. Betz, R. W. Blob, K. Fezzaa, W. J. Cooper, and W.-K. Lee, "Tracheal respiration in insects visualized with synchrotron X-ray imaging," *Science*, vol. 299, no. 5606, pp. 558–560, 2003.

[14] R. Xuan, X. Zhao, D. Hu, J. Jian, T. Wang, and C. Hu, "Three-dimensional visualization of the microvasculature of bile duct ligation-induced liver fibrosis in rats by X-ray phase-contrast imaging computed tomography," *Scientific Reports*, vol. 5, Article ID 11500, 2015.

[15] A. Bravin, P. Coan, and P. Suortti, "X-ray phase-contrast imaging: from pre-clinical applications towards clinics," *Physics in Medicine and Biology*, vol. 58, no. 1, pp. R1–R35, 2013.

[16] C. A. Edwards and P. J. Bohlen, *Biology and Ecology of Earthworms*, Springer, 1996.

[17] C. A. Edwards, *Earthworm Ecology*, CRC Press, 2004.

[18] K. E. Lee, *Earthworms: Their Ecology and Relationships With Soils and Land Use*, Academic Press, Sydney, Australia, 1985.

[19] H. Xie, B. Deng, G. Du et al., "X-ray biomedical imaging beamline at SSRF," *Journal of Instrumentation*, vol. 8, no. 8, Article ID C08003, 2013.

[20] R. Chen, P. Liu, T. Xiao, and L. X. Xu, "X-ray imaging for non-destructive microstructure analysis at SSRF," *Advanced Materials*, vol. 26, no. 46, pp. 7688–7691, 2014.

[21] R. C. Chen, H. L. Xie, L. Rigon, R. Longo, E. Castelli, and T. Q. Xiao, "Phase retrieval in quantitative X-ray microtomography with a single sample-to-detector distance," *Optics Letters*, vol. 36, no. 9, pp. 1719–1721, 2011.

[22] R. C. Chen, L. Rigon, and R. Longo, "Quantitative 3D refractive index decrement reconstruction using single-distance phase-contrast tomography data," *Journal of Physics D: Applied Physics*, vol. 44, no. 49, Article ID 495401, 2011.

[23] R.-C. Chen, D. Dreossi, L. Mancini et al., "PITRE: software for phase-sensitive X-ray image processing and tomography reconstruction," *Journal of Synchrotron Radiation*, vol. 19, no. 5, pp. 836–845, 2012.

[24] A. P. Almeida, D. Braz, L. P. Nogueira et al., "Phase contrast X-ray microtomography of the Rhodnius prolixus head: comparison of direct reconstruction and phase retrieval approach," *Radiation Physics and Chemistry*, vol. 95, pp. 243–246, 2014.

[25] X. Wu, H. Liu, and A. Yan, "Phase-contrast X-ray tomography: contrast mechanism and roles of phase retrieval," *European Journal of Radiology*, vol. 68, no. 3, supplement, pp. S8–S12, 2008.

[26] R. A. Harris, D. H. Follett, M. Halliwell, and P. N. T. Wells, "Ultimate limits in ultrasonic imaging resolution," *Ultrasound in Medicine and Biology*, vol. 17, no. 6, pp. 547–558, 1991.

[27] J. B. Aguayo, S. J. Blackband, J. Schoeniger, M. A. Mattingly, and M. Hintermann, "Nuclear magnetic resonance imaging of a single cell," *Nature*, vol. 322, no. 6075, pp. 190–191, 1986.

[28] T. Wilson, *Confocal Microscopy*, vol. 426, Academic Press, London, UK, 1990.